Statistics of major Chilean earthquakes recurrence

Virginia Silbergleit & Claudia Prezzi

Natural Hazards
Journal of the International Society for the Prevention and Mitigation of Natural Hazards

ISSN 0921-030X
Volume 62
Number 2

Nat Hazards (2012) 62:445-458
DOI 10.1007/s11069-012-0086-8

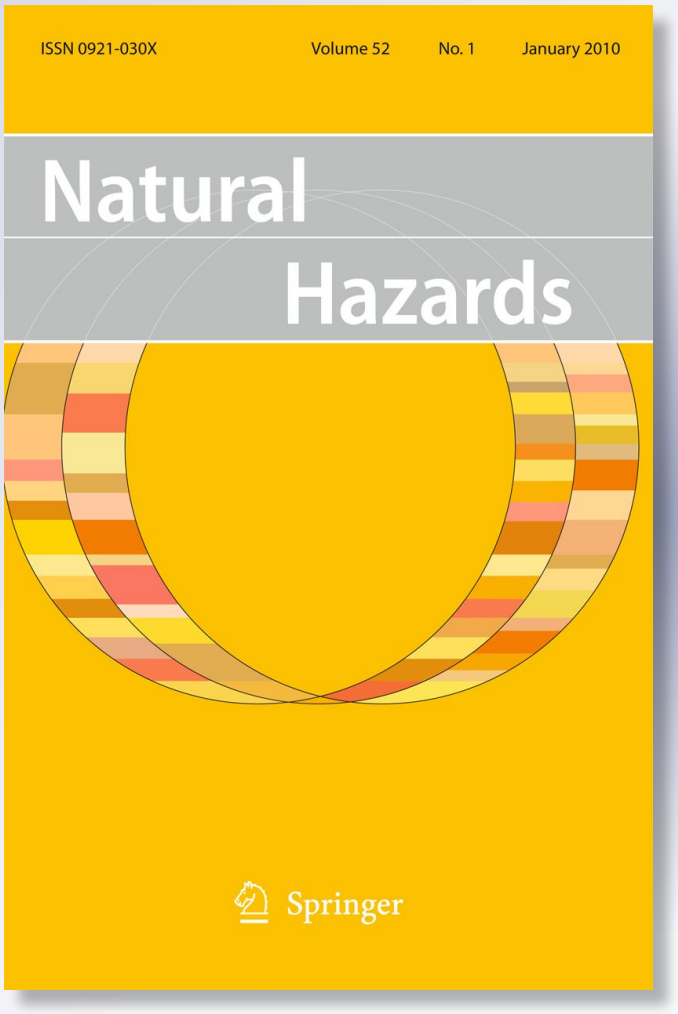

Springer

Nat Hazards (2012) 62:445–458
DOI 10.1007/s11069-012-0086-8

ORIGINAL PAPER

Statistics of major Chilean earthquakes recurrence

Virginia Silbergleit · Claudia Prezzi

Received: 9 August 2011 / Accepted: 5 January 2012 / Published online: 8 February 2012

Abstract In this work, we consider historical earthquakes registered in Chile (from 1900 up to 2010) with epicenters located between 19 and 40°S latitude, in order to evaluate the probabilities of the occurrence of strong earthquakes along Chile in the near future. Applying Gumbel's technique of first asymptotic distribution, Wemelsfelder's theory and Gutenberg–Richter relationship, we estimate that during the next decade strong earthquakes with Richter magnitudes larger than 8.7–8.9 could occur along Chile. According to our analysis, probabilities for the occurrence of such a strong earthquake range between 64 and 46% respectively. Particularly in the very well known "seismic gap" of Arica, a convergence motion between Nazca and South American plates of 77–78 mm/year represents more than 10 m of displacement accumulated since the last big interplate subduction earthquake in this area over 134 years ago. Therefore, this area already has the potential for an earthquake of magnitude >8.

Keywords Major Chilean earthquakes · Nazca plate · South American plate · Statistical analysis

1 Introduction

The Andean Cordillera with its active volcanoes and the large earthquakes registered along the coast of South America are dramatic manifestations of plate convergence (Norabuena et al. 1998). Eight events with magnitudes greater than 8 have taken place only during the twentieth century. This extreme seismicity (one of the largest around the world) is a

V. Silbergleit (✉)
Facultad de Ingeniería, CONICET-Universidad de Buenos Aires, Av. Las Heras 2214, C1127AAR, C.A.B.A, Buenos Aires, Argentina
e-mail: vsilbergleit@fi.uba.ar

C. Prezzi (✉)
Dpto. de Cs. Geológicas, FCEyN, IGEBA, CONICET-Universidad de Buenos Aires, Ciudad Universitaria, Pabellón 2, 1428, C.A.B.A. Buenos Aires, Argentina
e-mail: prezzi@gl.fcen.uba.ar

consequence of the subduction of the oceanic Nazca Plate below South America at a rate of about 65–78 mm/year (e.g., Angermann et al. 1999; Somoza and Ghidella 2005). Various geophysical studies and models published recently (e.g., Lindo et al. 1992; Schurr et al. 2003; Tassara et al. 2006; Heit et al. 2008; Prezzi et al. 2009) tried to achieve a detailed image of the geometry of this subduction zone, in an intend to accomplish a better understanding of the seismogenic processes and associated hazards.

The Nazca Plate has a homogeneous composition with high density rocks and is easily bent. However, notable differences in seismicity exist along this subduction zone. For example, the area extending between 35°S and 37°S, where the 8.8 magnitude 2010 earthquake took place, is located to the north of the rupture zone associated with the large 1960 event of 9.5 magnitude (Cifuentes 1989) and to the south of the rupture zones corresponding to the 1928 Talca earthquake of 7.1 magnitude (Beck et al. 1998), and the 1906 and 1985 Valparaiso earthquakes of 7.9 and 7.5 magnitude, respectively (Barrientos 1995). On the other hand, Cisternas and Vera (2008) studied the Magallanes seismicity in southern Chile, indicating that there is a relative lack of seismic activity in Magallanes in comparison with the regions to the north. Nevertheless, two main historical earthquakes (of 7.5) occurred in 1879 and 1949 in Magallanes. Moreover, Sparkes et al. (2010) showed that the maximum rupture length, and hence magnitude, of large subduction earthquakes is determined by the size and lateral spacing of subducted topography with relief >800–1,000 m. The subduction of seafloor relief >800–1,000 m impedes or stops earthquake rupture. The length of margin sectors with subducted relief <800 m (where rupturing is unimpeded) might impose an upper limit to the earthquake size (Sparkes et al. 2010). According to Sparkes et al. (2010), rupture lengths between Nazca and Juan Fernández Ridges (Fig. 1) would be no larger than 550 km, consequently the largest earthquakes along this sector would have moment magnitudes no larger than 9.1. On the other hand, rupture would be unimpeded to the south of Juan Fernández Ridge (between approximately 35–45°S) over a length of 1,450 km, enabling earthquake ruptures 33% longer than in the 1960 moment magnitude 9.5 event (Sparkes et al. 2010).

The Gumbel's asymptotic distributions were successfully applied by Siscoe (1976) and Silbergleit (1998) to the study of sunspots and geomagnetic storms respectively. Burton and Makropoulos (1985) examined the relationship between assessments of seismic risk using Gumbel's third asymptotic distribution ("part process" statistical model) and that obtained applying the Gutenberg–Richter relationship ("whole process" technique), concluding that both methods provide a mutually compatible description of the seismic features of a region. The extreme value method has obvious advantages as far as the requisite data are concerned (the largest earthquakes) when compared with methods requiring the whole data set (all earthquakes), which is rarely completely reported. Burton and Makropoulos (1985) demonstrated the existence of a clear consistency with the stability postulate from which asymptotic distributions of extremes are deduced, providing further confidence in this method. Kulikov et al. (2005) also applied the theory of Extreme Statistics to determine earthquakes return periods for tsunamigenic seismic events occurring along the coasts of Perú and northern Chile. Barrientos (2007) noted that return periods for magnitude 8 events are of the order of 80–130 years for any region in Chile, but about 12 years when the country is considered as a whole. Ruegg et al. (2009) stated that a major earthquake of magnitude larger than 8 is registered every 10 years in Chile.

In our work, we consider historical earthquakes occurred in Chile (from 1900 up to 2010) with epicenters located between 19 and 40°S latitude and a Richter magnitude >7 (Table 1). Events older than 1900 have not been included in the analysis because data prior to 1900 are deficient and uncertain (e.g., Kulikov et al. 2005).

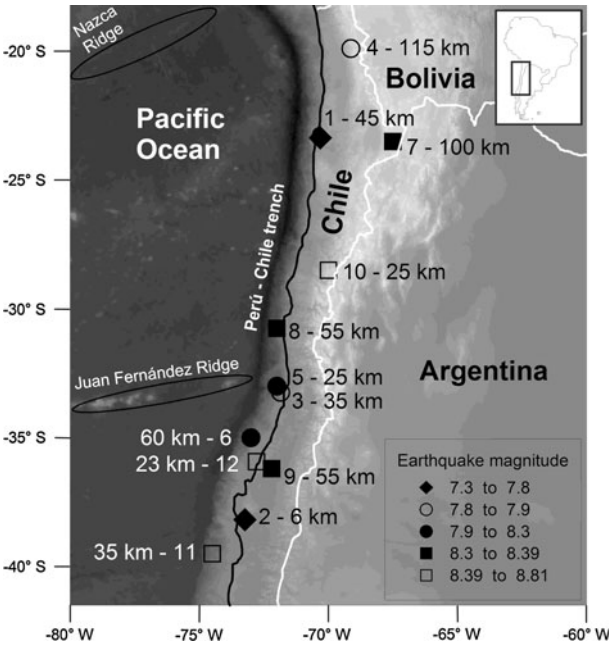

Fig. 1 Shaded relief topography map of the studied area showing the location, Richter magnitude and hypocenter depth (km) of the earthquakes presented in Table 2. The *numbers* next to the *symbols* correspond to the earthquakes numbers used in the first column of Table 2. *White line*: political boundaries, *black line*: coast line. *Black ellipses*: Nazca and Juan Fernández Ridges, which are considered to be the most important topographic features determining the segmentation and the seismogenic zones along Chile. Rupture length between Nazca and Juan Fernández Ridges would be no larger than 550 km, consequently the largest earthquakes along this sector would have moment magnitudes no larger than 9.1

We applied Gumbel's (1967) theory, Wemelsfelder's (1961) approach and Gutenberg and Richter (1954) relationship. The major goal of this paper is to explore the probability of a major earthquake occurrence in Chile during the next decade.

2 Seismogenic zones along Chile

Seismogenic zones are well-defined and classified in Chile. Large shallow (0–50 km depth) thrust earthquakes occur along the coast associated to the coupled region between the Nazca and South American Plates; large deeper (70–100 km depth) tensional and compressional earthquakes take place within the subducting plate; and very shallow seismicity (0–20 km depth) is registered in some specific zones as the cordillera region of Central Chile and the southern Magallanes Strait (Barrientos 2007).

Barrientos (2007) also identified and characterized different seismogenic regions along the Perú—Chile subduction zone:

(a) Arica—Tocopilla (17–22°S): Nishenko (1985) characterized this region as a seismic gap. The southern part of this zone (Mejillones Península to Paposo) was reactivated in 1995 with an earthquake of 7.3 magnitude (event number 1 in Table 2; Fig. 1). On the northern extreme of this region, a major earthquake was registered in Perú in

Table 1 Earthquakes considered in the present article

Date	Local time	ELA	ELO	*M*
8/16/1906	19:48	−33	−72	7.9
6/8/1909	1:00	−26.5	−70.5	7.6
10/4/1910	19:00	−22	−69	7.3
9/15/1911	8:10	−20	−72	7.3
1/29/1914	23:30	−35	−73	8.2
2/14/1917	20:48	−30	−73	7
5/20/1918	12:57	−28.5	−71.5	7.9
12/4/1918	7:47	−26	−71	8.2
3/1/1919	23:37	−41	−73.5	7.2
3/2/1919	7:45	−41	−73.5	7.3
12/10/1920	0:25	−39	−73	7.4
11/7/1922	19:00	−28	−72	7
11/10/1922	23:53	−28.5	−70	8.39
5/4/1923	17:47	−28.75	−71.75	7
5/15/1925	7:18	−26	−71.5	7.1
4/28/1926	7:13	−24	−69	7
11/21/1927	19:17	−44.5	−73	7.1
11/20/1928	16:35	−22.5	−70.5	7.1
12/1/1928	0:06	−35,000	−72,000	8.3
10/19/1929	16:18	−23	−69	7.5
3/18/1931	4:02	−32.5	−72	7.1
2/23/1933	4:09	−20	−71	7.6
3/1/1936	17:45	−40	−72.5	7.1
7/13/1936	7:12	−24.5	−70	7.3
1/25/1939	23:32	−36.2	−72.2	8.3
4/18/1939	2:22	−27	−70.5	7.4
10/11/1940	14:41	−41.5	−74.5	7
7/8/1942	1:55	−24	−70	7
3/14/1943	14:37	−20	−69.5	7.2
4/6/1943	12:07	−30.75	−72	8.3
12/1/1943	6:34	−21	−69	7
7/13/1945	7:17	−33.25	−70.5	7.1
8/2/1946	15:19	−26.5	−70.5	7,9
4/19/1946	23:29	−38	−73.5	7.3
4/25/1949	9:54	−19.75	−69	7.3
5/29/1949	21:32	−22	−69	7
12/17/1949	2:53	−54	−71	7.8
12/17/1949	11:07	−54	−71	7.8
1/29/1950	20:56	−53.5	−71.5	7
12/9/1950	17:38	−23.5	−67.5	8,3
5/6/1953	13:16	−36.5	−72.6	7,6
12/6/1953	22:05	−22.1	−68.7	7.4
2/8/1954	–	−29,000	−70,500	7,7

Table 1 continued

Date	Local time	ELA	ELO	*M*
4/19/1955	16:24	−30	−72	7.1
1/8/1956	16:54	−19	−70	7.1
12/17/1956	22:31	−25.5	−68.5	7
7/29/1957	13:15	−23.5	−71.5	7
6/13/1959	20:12	−20.42	−69	7.5
5/21/1960	6:02	−37.5	−73.5	7.3
5/22/1960	6:32	−37.5	−73	7.3
5/22/1960	15:11	−39.5	−74.5	8.5
6/19/1960	22:01	−38	−73.5	7.3
11/1/1960	4:45	−38.5	−75.1	7.4
7/13/1961	17:19	−41.7	−75.2	7
2/14/1962	2:36	−37.8	−72.5	7.3
8/3/1962	4:56	−23.3	−68.1	7.1
2/23/1965	18:11	−25.67	−70.63	7
3/28/1965	12:33	−32.418	−71.1	7.4
12/28/1966	4:18	−25.51	−70.74	7.8
3/13/1967	12:06	−40.12	−74.68	7.3
12/21/1967	22:25	−21.8	−70	7.5
6/17/1971	17:00	−25.402	−69.058	7
7/8/1971	23:03	−32.511	−71.207	7.5
8/18/1974	6:44	−38.453	−73.431	7.1
5/10/1975	10:27	−38.183	−73.232	7.7
11/29/1976	21:40	−20.52	−68.919	7.3
8/3/1979	14:11	−26.518	−70.664	7
10/16/1981	0:25	−33.134	−73.074	7.5
10/4/1983	14:52	−26.535	−70.563	7.3
3/3/1985	19:46	−33.24	−71.85	7.8
4/8/1985	21:56	−34.131	−71.618	7.5
3/5/1987	6:17	−24.388	−70.161	7.3
8/8/1987	11:48	−19	−70	7.1
7/30/1995	1:11	−23.36	−70.31	7.3
6/13/2005	18:44	−19.895	−69.125	7.8
2/27/2010	3:34	−36.29	−73.239	8.8

M refers to Richter magnitude, calculated from surface seismic waves. ELA and ELO are the epicenter latitude and longitude, respectively. The data were downloaded from http://ssn.dgf.uchile.cl/home/terrem.html by the Seismological Service of the University of Chile)

2001. Its rupture region extended up to southern Perú. Consequently, a stretch of approximately 500 km along southern Perú—northern Chile (Ilo—Arica—Mejillones Península) did not suffer significant earthquakes since 1868–1877 (Barrientos 2007). Barrientos (2007) noted that seismicity in this region also takes place when the subducting slab undergoes normal faulting at about 100 km depth (e.g., event number 4 in Table 2; Fig. 1).

(b) Antofagasta—Taltal (22–25°S): The 1995 Antofagasta earthquake (event number 1 in Table 2; Fig. 1) is one of the best studied events in Chile, with an estimated hypocenter depth of approximately 45 km. As is the case to the north, extension takes place along the subduction zone. A significant extensional event occurred in 1950 at 100-km depth (event number 7 in Table 2; Fig. 1).

Table 2 Largest earthquake per decade and the corresponding probability value considered in the present article

	M	ELA	ELO	Depth (km)	Probability	Plotting value
1	7.3	−23.36	−70.31	45	4.62E−02	−1.123199
2	7.7	−38.183	−73.232	6	1.29E−01	−7.18E−01
3	7.8	−33.24	−71.85	35	2.11E−01	−4.41E−01
4	7.8	−19.895	−69.125	115	2.94E−01	−2.03E−01
5	7.9	−33	−72	25	3.76E−01	2.27E−02
6	8.2	−35	−73	60	4.59E−01	2.49E−01
7	8.3	−36.2	−72.2	100	5.41E−01	4.88E−01
8	8.3	−30.75	−72	55	6.24E−01	7.51E−01
9	8.3	−23.5	−67.5	55	7.06E−01	1.056252
10	8.39	−28.5	−70	25	7.89E−01	1.43856
11	8.5	−39.5	−74.5	35	8.71E−01	1.98207
12	8.8	−36.29	−73.23	23	9.54E−01	3.051116

M refers to Richter magnitude, calculated from surface seismic waves. ELA and ELO are the epicenter latitude and longitude, respectively. The data were downloaded from http://ssn.dgf.uchile.cl/home/terrem.html by the Seismological Service of the University of Chile). Depth refers to the hypocenters depths

(c) Copiapó (26–29°S): This region was the site of major earthquakes in 1819 and 1922. Lockridge (1985) documented that the 1922 earthquake (event number 10 in Table 2; Fig. 1) generated a local tsunami with maximum wave heights of 9 m. The northern part of this event rupture zone was partially reactivated in 1983 with an earthquake with a hypocenter depth of 38 km. Comte et al. (2002) determined that the Wadati–Benioff zone in the coupled region has an average dip angle of 20°, similar to the ones calculated for other areas of Chile.

(d) La Serena—La Ligua (30–33°S): An underthrusting mechanism was proposed for the 1943 event (event number 8 in Table 2; Fig. 1) (Beck et al. 1998). In 1997, an intraplate earthquake took place. It was the result of a nearly vertical fault with rupture initiation at 68 km depth. Pardo et al. (2002) postulated that it was probably the result of the unbending of the Nazca plate when reaching subhorizontality to the east. The region between 27 and 33°S shows a gradual southward subhorizontalization of subduction and a lack of recent volcanism (Barrientos 2007), unlike to the north and south. Such changes in dip angle are only noticeable when the subducting slab reaches depths of approximately 100 km. Therefore, the initial part of the subduction (0–50 km) has similar dip angle from 18.5 to 46°S.

(e) Valparaíso—Pichilemu (33–35°S): The 1906 (event number 5 in Table 2; Fig. 1) and 1985 (event number 3 in Table 2 and Fig. 1) earthquakes in central Chile correspond to the sequence that has been taking place regularly in the region every 82 ± 6 years (Barrientos 2007). Both events present offshore epicenter location, rupture lengths of over 150 km, coastal uplift and small tsunamis. Pardo et al. (2002) concluded that the maximum area involved in the 1985 event rupture included a region of 200 km by 90 km, with most activity within 10 and 45 km depth. Shallow seismicity has also been detected in this region (less than 20-km depth) in the Andes. Santiago area is exposed to the effects of relatively large intermediate-depth (80–110 km) tensional—type earthquakes. Barrientos et al. (1997) estimated recurrence periods of 110 years for 7.5 magnitude intermediate-depth earthquakes between 32 and 37°S.

(f) Pichilemu—Concepción (35–37°S): The 1939 Chillán event (event number 9 in Table 2; Fig. 1) has been the most disastrous earthquake in terms of human life in Chile in historical times. A hypocenter depth of 60 km was estimated. Two other areas of seismicity are at shallow depths near the volcanic zone and under the Central Valley (Barrientos 2007). In 2010, a moment magnitude 8.8 earthquake ruptured the Nazca and South American plate boundary at a depth of about 35 km, causing a displacement of approximately 10–14 m (event number 12 in Table 2; Fig. 1). This event broke a 550–600 km long, 100 km wide segment of the plate interface and lies between two earlier major earthquakes: 1985 Valparaiso to the north (event number 3 in Table 2; Fig. 1) and 1960 Valdivia to the south (event number 11 in Table 2; Fig. 1). This 2010 event filled a "seismic gap" previously identified by Ruegg et al. (2009). Seismic gaps are regions that have not ruptured for some time and are therefore considered "overdue." The last great earthquake to rupture in this region was in 1835, thereby this quake released almost 175 years of accumulated seismic energy. Ruegg et al. (2009) suggested that the accumulated seismic energy in the gap was enough to release a moment magnitude 8.0–8.5 earthquake.

(g) Arauco Península—Taitao Península (38–45°S): The megathrust earthquake of 1960 (event number 11 in Table 2; Fig. 1) was the largest event recorded in the last century. The total rupture length is of the order of 1,000 km with 20–40 m of displacement and a hypocenter depth of approximately 35 km. Plafker and Savage (1970) proposed that these types of event recur every 400 years. On the other hand, Cisternas (2005) estimated a mean recurrence of the order of 280 years.

3 Prediction techniques

3.1 Gumbel's theory

As it was noted by Kulikov et al. (2005), data prior to 1900 are deficient and uncertain. The recent Maule and Arauco earthquake clearly influence the statistical results because Gumbel's technique considers extreme values and the biggest of them have an important role on the predicted extreme magnitudes.

We applied Gumbel's technique of first asymptotic distribution because it is one of the most used for predicting events in different fields such as seismology. The extreme value method has the advantage of using only the most certain observed data (the largest ones for every period in a selected time scale).

For each decade, the strongest earthquakes registered along Chile were selected (see Fig. 1; Table 2). The details of this method were published by Gumbel (1967). According to Gumbel (1967), for a given maximum observation, the probability that its value was less than M is defined as $P = \Psi(M)$. The probability that its value was equal or greater than M is given by $P = [1 - \Psi(M)]$.

The theory of extremes gives the mathematical expression of $\Psi(M)$ (Gumbel 1967):

$$\Psi(M) = \exp\{-\exp[-(\alpha + \beta M)]\} = \exp\{-\exp[-A\,(M - \mathrm{mo})]\} \quad (1)$$

where α, β, A and mo are constants defined by $\beta = A$ and $\alpha = -A \times \mathrm{mo}$.

A, α, β and mo (the mode) are determined by a linear square fit shown in Fig. 2.

As the probability function for the maximum amplitude is not known, the values of $\Psi(M)$ are estimated by using the Gringorten (1963) rule. For N observed extreme values, the relationship between $\Psi(M)$ and M is obtained.

Extreme M are calculated considering earthquakes registered between the years 1900 and 2010 (see Fig. 1) and using the maximum Richter magnitude (M) per decade in ascending order: $M1 < M2 < \ldots <$ M12. Earthquakes occurred prior to 1900 are not considered in our analysis taking into account the uncertainties and deficiencies of such data. To obtain good results, we must use certain values as input data.

To estimate $\Psi(M)$, the statistics procedure of Gringorten (1963) is considered. For each observed peak value, the following probability is assigned:

$$\mathrm{Pi} = (i - 0.44)/(N + 0.12) \tag{2}$$

where i is the ordinal number and N (number of decades considered) is equal to 12, (Siscoe 1976). By considering Eq. 2, the related Gi values are defined by:

$$\mathrm{Gi} = -\ln[-\ln(\mathrm{Pi})] \tag{3}$$

Pi and Gi values are mathematical tools useful to estimate $\Psi(M)$. Figure 2 shows the results obtained by Eqs. 2 and 3. Through the linear fit of Eq. 3, the mathematical expression of $\Psi(M)$ is obtained.

The return periods $T(M)$ and $t(M)$ are calculated by using the expressions:

$$T(M) = [1 - \Psi(M)]^{-1} \tag{4}$$

$$t(M) = [\Psi(M)]^{-1} \tag{5}$$

The increment of the expected range of extremes values as a function of the number of decades (periods) in a set can be found from Eq 4. $T(M)$ is the expected number of decades required to have one period with its extreme equal to or exceeding M. The expression $t(M) = [\Psi(M)]^{-1}$ represents the expected number of periods necessary to have one of them with its extreme less than M. These functions are plotted in Fig. 3, in which the number of decades from 1900 is shown as the ordinates. For each decade (K), both bounds are determined by $K = T(M)$ and $K = t(M)$, as they are presented in Fig. 3.

On average, for two decades, one value will be larger and one value will be smaller than the median (mv). The median corresponds to the abscissa value for the point in which $T(M) = t(M) = 2$, then mv = 8.2 is obtained from Fig. 3.

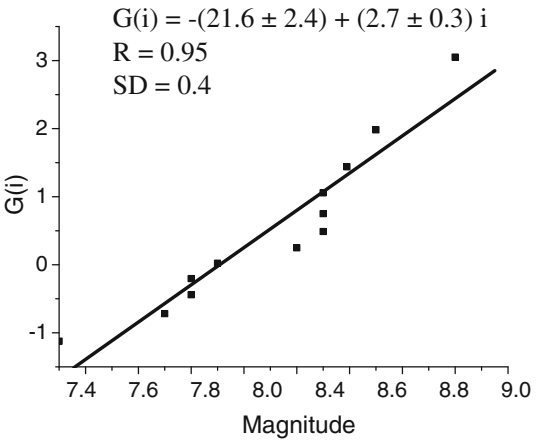

Fig. 2 Squares indicate the results obtained by Eq. 3. R and SD are the coefficient of correlation and the average error, respectively

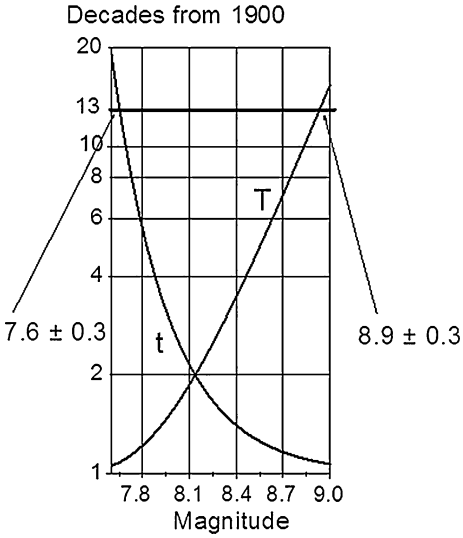

Fig. 3 The ascending branch shows the number of decades that would be required to register an earthquake with extreme value equal to or exceeding *M*. The descending one exhibits the number of decades that would be necessary to detect an earthquake with extreme value less than *M*

According to Gumbel (1967), the arithmetic mean (am), which is the average of all results, is related to the standard deviation by SD = 1.2825/*A* (Siscoe 1976 and Silbergleit 1998), where the constant *A* is defined by Eq. 1.

The scatter is called Rd (relative dispersion), and it is calculated dividing SD by the mode (mo).

The statistical parameters characteristic of extreme values are as follows: the mode (mo = 8.0) and the mean (am = 8.1), with SD = 0.48 and Rd = 0.06.

3.2 Wemelsfelder's approach

The most important difference between Gumbel's and Wemelsfelder's theory lies in the initial handling of available data. Instead of picking the largest earthquake registered for each decade, Wemelsfelder proposed to count the number of exceedences of large earthquakes in the entire period of observations (100 years). Having counted the number of exceedences, the yearly rate (or the number per year) is plotted versus the corresponding earthquake magnitude. Such plot is called a frequency curve (Fig. 4). The abscissa gives the number N of the times each magnitude has been exceeded, reduced to the number per year. For practical reasons, the scale of the abscissa is logarithmic. It is important to note that this procedure leads to a fairly straight curve (Fig. 4). Obviously, the frequency curve cannot end abruptly at the highest observed magnitude. An extrapolation of straight character is carried out for the levels which will be of interest for this investigation. Assuming that strong earthquakes are rare and independent events, Wemelsfelder applied the Poisson probability law. According to this law, the probability of exceeding a magnitude (*M*) in a period of *T* years is as follows:

$$q = 1 - e^{-mT} \tag{6}$$

where the parameter *m* is the rate of exceedence, which can be estimated from the frequency curve. For the straight frequency curve, the following equation applies (Fig. 4):

$$m = e^{[(6.93-M)/0.39]} \tag{7}$$

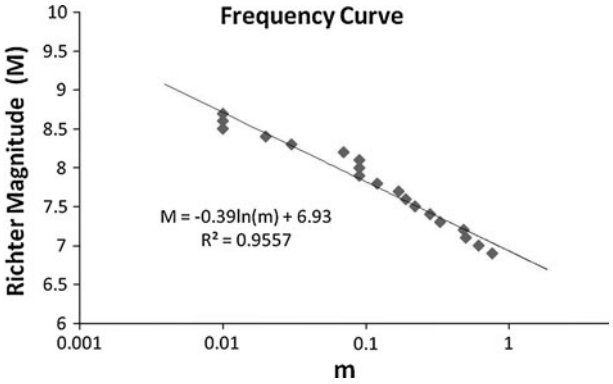

Fig. 4 Frequency curve of Richter magnitude of earthquakes between 1900 and 2010. The best fitting logarithmic regression line, the corresponding equation and R^2 parameter are shown

3.3 Gutenberg—Richter relationship

The Gutenberg and Richter (1954) law expresses the relationship between the magnitude and total number of earthquakes in any given region and time period of at least that magnitude. It is defined by:

$$\log N(M) = a - b\,M \tag{8}$$

where $N(M)$ is the number of earthquakes of magnitude greater than M, and the parameters a and b are constants, which characterize the studied zone. The constant b is typically equal to 1.0 in seismically active regions. This means that for every magnitude 4.0 event, there will be 10 magnitude 3.0 quakes and 100 magnitude 2.0 quakes. There is some variation with b-values in the range 0.5–1.5 depending on the tectonic environment of the region. The a-value is of less scientific interest and simply indicates the total seismicity rate of the region. a and b are obtained from Fig. 5. Their values are as follows: $a = 9.59 \pm 0.99$ and $b = 1.21 \pm 0.12$. Figure 5 shows the result of the least squares fit obtained for the sample considered.

4 Results

Figure 3 depicts the return period versus earthquake magnitude obtained applying Gumbel's technique of first asymptotic distribution, the upper and lower bounds are shown for 13 decades. It is expected to observe one value outside to the right and one outside to the left of the defined bounds (see Fig. 3). The Richter magnitude of the earthquake that took place on July 30, 1995, is less than 7.6 (event number 1 in Table 2; Fig. 1), then the other value out of the interval will be greater than the upper bound. According to these results, during the next decade, it is expected that an earthquake with a Richter magnitude higher than 8.9 would occur.

Regarding Wemelsfelder's theory, we calculated that the probability of the occurrence of an earthquake with a Richter magnitude (M) exceeding 8.9 would be of 46%, while such probability for earthquakes exceeding 8.8 and 8.7 M would be of 55 and 64% respectively. Following the division of the range of possibilities made by Wemelsfelder (1961) and

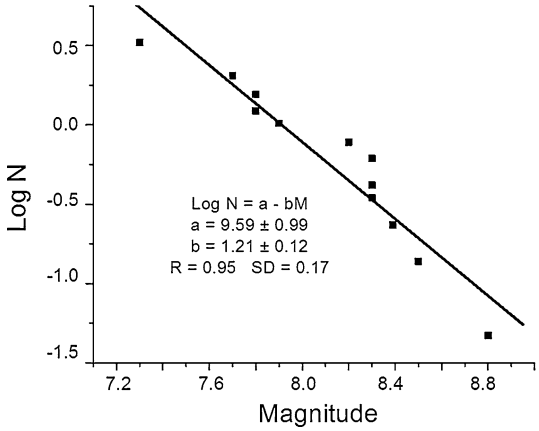

Fig. 5 Gutenberg–Richter law for the studied earthquakes. The best fitting regression line, the corresponding equation and a, b, R^2 and SD parameters are shown

considering the corresponding values of m, an 8.7 M earthquake would represent a remarkable maximum, while 8.8, 8.9 and 9.0 M earthquakes would represent exceptional maxima. Remarkable maxima occur at a rate of 1 in 10. An exceptional maximum is a phenomenon presenting itself at a rate of 1 in 100 only (Wemelsfelder 1961).

In the case of Gutenberg–Richter law, the most probable maximum magnitude detected in a time scale of 10 years is equal to $a/b = 7.9 \pm 1.6$. This magnitude interval coincides with the results obtained applying Gumbel's and Wemelsfelder's theories.

Consequently, the obtained values indicate that a Chilean earthquake greater than the prior ones (observed during the last 120 years) could occur during the next 10 years.

5 Discussion

Barrientos (2007) stated that potential areas most subject to large—magnitude earthquakes are above the coupling zone between the Nazca and South American Plates, which corresponds to the contact region between the trench and approximately 45–53 km depth along the Wadati–Benioff zone. Such events correspond to low-angle thrust earthquakes distributed along the coast. This author also noted that further inland intraplate earthquakes occur within the subducting Nazca Plate. These events are characterized by tensional mechanisms, depths of the order of about 70–80 km and higher stress drops. They usually produce higher accelerations at the surface. These intraplate earthquakes can reach magnitudes of about 8 and are also included in our statistical analysis.

Considering the location and characteristics of the major seismic events described and used in this paper and previously published research (e.g., Barrientos 2007; Socquet et al. 2008; Vigny 2010; Shen-Tu and Mahdyiar 2010), a "seismic gap" is identified in northern Chile in the coupling zone between Nazca and South American Plates, which seems mature for an imminent earthquake. Such gap is named as "the Arica gap," where the last giant earthquakes occurred in 1868 (with a moment magnitude estimated at 8.8) and in 1877 (Tarapacá earthquake, with an estimated moment magnitude of 8.3). Considering that the convergence motion between Nazca and South American plates is of 77 mm/year with an azimuth of 75.7°N at 17°S and of 78 mm/year with an azimuth of 74°N at 22°S (Somoza and Ghidella 2005), in the worst case scenario, more than 10 m of displacement accumulated in this area during the last 134 years. Following Ruegg et al. (2009), such slip

deficit would be large enough to generate the potential for an earthquake of moment magnitude >8–8.5. On the other hand, Sparkes et al. (2010) documented that in the area of "the Arica gap," the length of margin sections with subducted relief <800 m, which unimpedes great earthquakes rupturing, would impose an upper bound on the possible earthquake size. These authors proposed that the largest earthquakes in the Arica area would have rupture lengths no larger than 550 km, predicting maximum moment magnitudes of 9.1.

The earthquake cycle is divided into three intervals: interseismic, coseismic (the major earthquakes) and postseismic interval. In the interseismic interval, stress builds up and produces seismicity. In the postseismic interval, aftershocks and aseismic deformation occur. The stress change produced by postseismic deformation might influence earthquake risk estimate in a wide spatial and temporal domain (Wang 2010). Casarotti and Piersanti (2003) showed that two seismic gaps near southern Perú and northern Chile are stressed by postseismic relaxation following the megaearthquakes in the past 60 years. Lin and Stein (2004) examined stress changes on the rupture surface imparted by the 1995 moment magnitude 8.1 Antofagasta earthquake (event number 1 in Table 2; Fig. 1). These authors calculated the coseismic Coulomb stress change on the fault surface and compared it to the principal aftershocks and site of postseismic slip. They determined that calculated Coulomb stress increases of 2–20 bars correspond closely to sites of aftershocks and postseismic slip, whereas aftershocks are absent where the stress drops by more than 10 bars. The 1995 Antofagasta subduction event increased the Coulomb stress north of the rupture. Lin and Stein (2004) observed that aftershocks extended farthest from the north end of the rupture, where the off-fault stress changes were greatest. These authors documented that the 1995 Antofagasta subduction event increased the Coulomb stress north of the rupture more than to the south, and so subsequent events are more likely to occur to the north. Wang (2010) carried out an analysis of postseismic processes and a Coulomb stress modeling of the 1995 Antofagasta event. This author suggested that the co- and postseismic stresses induced by the Antofagasta earthquake could have encouraged the occurrence of the moment magnitude 7.8 2007 Tocopilla event, which ruptured the seismic gap to the north over a distance of about 150 km, in the northern prolongation of the zone ruptured during the 1995 quake.

Recently, Chlieh et al. (2011) used about two decades of geodetic measurements to characterize interseismic strain build up along the Central Andes subduction zone. These authors determined that in northern Chile, interseismic coupling is very high and the rupture of the 2007 Tocopilla earthquake has released only 4% of the elastic strain that has accumulated since 1877. Interseismic coupling (ISC) is defined as the ratio of the slip deficit rate and the long-term slip rate (Chlieh et al. 2011). An ISC value of 1 corresponds to full locking, while an ISC of 0 corresponds to creeping at the long-term plate convergence rate. It is very interesting to determine the pattern of ISC on a megathrust fault and compare the cumulative rate of moment deficit in the interseismic period with the moment released by former earthquakes. The deficit of moment that has accumulated in northern Chile is equivalent to a moment magnitude 8.8 earthquake (Chlieh et al. 2011). A minimum moment magnitude of 8.6 is estimated when potential nonsteady state interseismic process is taken into account (Chlieh et al. 2011).

These observations are in accordance with our prediction of the probable occurrence during the next decade of an earthquake with a Richter magnitude higher than 8.7–8.9.

Therefore, the present analysis would be useful and could be taken into account to evaluate the possible occurrence of near future strong earthquakes along Chile (particularly in the Arica area) and their associated hazards.

6 Conclusions

Our statistical analyses suggest the possible occurrence of a major earthquake in Chile with a Richter magnitude >8.7–8.9.

Taking into account previous studies published by other authors, it is considered that "the Arica seismic gap" identified in northern Chile could be the locus of the occurrence of such a major earthquake.

The Richter magnitude predicted by our statistical analysis coincides with magnitudes predicted by other authors applying completely different methodologies.

The present analysis would be useful and could be taken into account to evaluate the possible occurrence of near future strong earthquakes along Chile (particularly in the Arica area) and their associated hazards.

Acknowledgements We are grateful to unknown referees for helpful comments and suggestions. This work was partially supported by 20020100100227 (UBACYT) of Facultad de Ingeniería, Universidad de Buenos Aires, 2010–2012 0266 and 2011–2013 0643 (UBACYT) of Facultad de Cs. Exactas y Naturales, Universidad de Buenos Aires, 11420090100258 and PIP 747 of CONICET of Argentina.

References

Angermann D, Klotz J, Reigber C (1999) Space-geodetic estimation of the Nazca-South America Euler vector. Earth Planet Sci Lett 171:329–334

Barrientos SE (1995) Dual seismogenic behavior: the 1985 Central Chile earthquake. Geophys Res Lett 22:3541–3544

Barrientos SE (2007) Earthquakes in Chile. In: Moreno T, Gibbons W (eds) The geology of Chile. The Geological Society, London, pp 21–114

Barrientos S, Kausel E, Campos J (1997) Sismicidad de profundidad intermedia y peligro sísmico en Santiago. VIIICongreso Geológico Chileno, Antofagasta

Beck S, Barrientos S, Kausel E, Reyes M (1998) Source characteristics of historic earthquakes along the central Chile subduction zone. J S Am Earth Sci 11:115–129

Burton P, Makropoulos K (1985) Seismic risk of Circum-Pacific earthquakes: II. Extreme values using Gumbel's third distribution and the relationship with strain energy release. Pure Appl Geophys 123:849–869

Casarotti E, Piersanti A (2003) Postseismic stress difussion in Chile and south Perú. Earth Planet Sci Lett 206(3–4):325–333

Chlieh M, Perfettini H, Tavera H, Avouac J, Remy D, Nocquet J, Rolandone F, Bondoux F, Gabalda G, Bonvalot S (2011) Interseismic coupling and seismic potential along the Central Andes subduction zone. J Geophys Res116. doi:10.1029/2010JB008166

Cifuentes IL (1989) The 1960 Chilean earthquake. J Geophys Res 94:665–680

Cisternas M (2005) Predecessors of the giant 1960 Chile earthquake. Nature 437:404–407

Cisternas A, Vera E (2008) Sismos históricos y recientes en Magallanes. Magallanía 36(1):43–51

Comte D, Haessler H, Dorbath L, Pardo M, Monfret T, Lavenu A, Pontoise B, Hello Y (2002) Seismicity and stress distribution in the Copiapo, northern Chile subduction zone using combined on- and off-shore seismic observations. Phys Earth Planets Int 132:197–217

Gringorten II (1963) A plotting rule for extreme probability paper. J Geophys Res 68:813–817

Gumbel EJ (1967) Statistics of extremes. Columbia University Press, NY, p 375

Gutenberg B, Richter CF (1954) Seismicity of earth and associated phenomena. Princeton University Press, Princeton, p 310

Heit B, Koulakov G, Asch G, Yuan X, Kind R, Alcocer-Rodriguez I, Tawackoli S, Wilke H (2008) More constraints to determine the seismic structure beneath the Central Andes at 21°S using teleseismic tomography analysis. J South Am Earth Sci 25:22–36

Kulikov EA, Rabinovich AB, Thomson RE (2005) Estimation of tsunami risk for the coasts of Peru and northern Chile. Nat Hazards 35:185–209

Lin J, Stein R (2004) Stress triggering in thrust and subduction earthquakes and stress interaction between the southern San Andreas and nearby thrust and strike-slip faults. J Geophys Res 109:B02303. doi: 10.1029/2003JB002607

Lindo R, Dorbath C, Cisternas A, Dorbath L, Ocola L, Morales M (1992) Subduction geometry in central Peru from a microseismicity survey: first results. Tectonophysics 205:23–29

Lockridge P (1985) Tsunamis in Peru–Chile. World Data Center for Solid Earth and Geophysics, Boulder, CO, Report SE-39

Nishenko SP (1985) Seismic potential for large and great interpolate earthquakes along the Chilean and southern Peruvian margins of South America: quantitative reappraisal. J Geophys Res 90:3589–3615

Norabuena E, Leffler-Griffin L, Mao A, Dixon T, Stein S, Sacks IS, Ocola L, Ellis M (1998) Space geodetic observations of Nazca-South America convergence across the Central Andes. Science 279:358–362

Pardo M, Comte D, Monfret T, Boroschek R, Astroza M (2002) The October 15, 1997 Punitaqui earthquake (Mw = 7.1): a destructive event within the subducting Nazca Plate in central Chile. Tectonophysics 345:199–210

Plafker G, Savage JC (1970) Mechanism of the Chilean earthquakes of May 21 and 22, 1960. Geol Soc Am Bull 81:1001–1030

Prezzi C, Götze H-J, Schmidt S (2009) 3D density model of the Central Andes. Phys Earth Planet Interiors 177:217–234

Ruegg JC, Rudloff A, Vigny C, Madariaga R, de Chabalier JB, Campos C, Kausel E, Barrientos S, Dimitrov D (2009) Interseismic strain accumulation measured by GPS in the seismic gap between Constitución and Concepción in Chile. Phys Earth Planet Interiors 175:78–85

Schurr B, Asch G, Rietbrock A, Trumbull R, Haberland C (2003) Complex patterns of fluid and melt transport in the central Andean subduction zone revealed by attenuation tomography. Earth Planet Sci Lett 215:105–119

Shen-Tu B, Mahdyiar M (2010) Earthquake risk in Chile after February 2010. Air Curr 08(10):4

Silbergleit VM (1998) On the statistics of maximum sunspot numbers. J Atmos Solar Terr Phys 60:1707–1710

Siscoe GL (1976) On the statistics of the largest sunspot number per solar cycle. J Geophys Res 81:6224–6226

Socquet A, Bejar M, Carrizo D, Armijo R, Vigny C, Ruegg J-C, deChabalier J-B, Nercessian A, Charade O, Simons M, Bonvalot S (2008) Accommodation of convergence in North Chile seismic gap: questions raised by 2007 Mw 7.7 Tocopilla earthquake. Eos trans AGU, Fall Meeting Suppl, Abstract G33D-04

Somoza R, Ghidella M (2005) Convergencia en el margen occidental de América del Sur durante el Cenozoico: subducción de las placas de Nazca, Farallón y Aluk. Revista de la Asociación Geológica Argentina 60:797–809

Sparkes R, Tilmann F, Hovius N, Hillier J (2010) Subudcted seafloor relief stops rupture in South American great earthquakes: Implications for rupture behavior in the 2010 Maule, Chile earthquake. Earth Planet Sci Lett 298:89–94

Tassara A, Götze H-J, Schmidt S, Hackney R (2006) Three-dimensional density model of the Nazca plate and the Andean continental margin. J GeophyS Res 111. doi:10.1029/2005JB003976

Vigny C (2010) 27 February 2010 concepción, Chile earthquake—status on scientific information. http://www.geologie.ens.fr/∼vigny/articles/Chili-Concepcion-Eq-1-UK.pdf

Wang L (2010) Analysis of postseismic processes: afterslip, viscoelastic relaxation and aftershocks. Ph.D. Thesis, Rurh University Bochum, Germany, pp 110

Wemelsfelder J (1961) On the use of frequency curves of storm floods. In: Proceedings seventh conference coastal engineers. Berkeley, California, USA, pp 617–632